Urban Climate 31 (2020) 100540

Contents lists available at ScienceDirect

Urban Climate

journal homepage: www.elsevier.com/locate/uclim

Inter-local climate zone differentiation of land surface temperatures for Management of Urban Heat in Nairobi City, Kenya

Emmanuel Matsaba Ochola[a,*], Elham Fakharizadehshirazi[b], Aggrey Ochieng Adimo[a], John Bosco Mukundi[a], John Mwibanda Wesonga[a], Sahar Sodoudi[b]

[a] Department of Landscape and Environmental Sciences, College of Agriculture, Jomo Kenyatta University of Agriculture and Technology, Kenya
[b] Department of Earth Sciences, Institute for Meteorology, Freie University Berlin, Germany

ARTICLE INFO

Keywords:
Local climate zone
Land surface temperature
Urban heat
Urban morphology
Microclimate

ABSTRACT

Rapid Urbanisation often leads to the formation of Urban Heat Island (UHI), which is believed to link to the characteristics of a city. Proper management of UHI, would, therefore, require recognition of the possible range of heat load increase. This paper presents results of inter-local climate zone (LCZ) differentiation of land surface temperature (LST) for the management of urban hotspots in Nairobi city. WUDAPT methodology and LST_Landsat_8_split_window toolbox were used to generate LCZ and LST maps, respectively. Nairobi LCZs had a unique thermal climate that showed statistically significant differences (< 0.05) in mean LSTs among typical LCZs. LST patterns exhibited sensitivity to building densities and heights, land cover types and surface wetness. Dry and Natural zones were more thermally responsive than wet and built-up zones. However, build-up LCZs with heavy industry, compact buildings, lightweight lowrise (slums) and large lowrise buildings were characterised with warmer LSTs while natural LCZs with water bodies, dense trees and sparsely built classes were associated with slightly lower LSTs. The findings further demonstrate and support the use of LCZs for the delimitation and investigation of the influence of complex urban morphology on local climate formation in an equatorial city like Nairobi.

1. Introduction

Urbanisation process and changes that occur in the landscape lead to infrastructure replacing open land and vegetation; Concrete surfaces replace vegetation-covered surfaces (Hashim and Hashim, 2016). In Nairobi the rapid urbanisation (Oyugi et al., 2017), led to a serial of environmental problems, especially the formation of higher temperatures inbuilt urban areas, and also in other studies, it has been shown to impact those of the surrounding rural surroundings (Stone and Rodgers, 2001). This phenomenon, which is generally known as the Urban Heat Island (UHI), is viewed as the most illustrative and recorded sign of climate modification in the current time of increasing urbanisation (Santamouris et al., 2007; Santamouris et al., 2017) as it is expected that by 2050 about 70% of the worldwide populace will live in urban territories with a resulting even greater urban sprawl. > 100,000 cities in developing

* Corresponding author.
E-mail addresses: ocholax@gmail.com (E.M. Ochola), fakharizade@zedat.fu-berlin.de (E. Fakharizadehshirazi), adimo@agr.jkuat.ac.ke (A.O. Adimo), jbmukundi@jkuat.ac.ke (J.B. Mukundi), jwesonga@agr.jkuat.ac.ke (J.M. Wesonga), sodoudi@zedat.fu-berlin.de (S. Sodoudi).

https://doi.org/10.1016/j.uclim.2019.100540
Received 27 March 2019; Received in revised form 26 September 2019; Accepted 26 September 2019

countries are expected to triple their built-up areas by 2030. Even in developed nations, urban areas will expand by 2.5 times, notwithstanding their little populace measure and a lower rate of populace development (Angel et al., 2005). As a result, forecasts indicate that average temperatures will continue to rise in the coming decades in most cities, mostly because of anthropogenic forcings (Oppenheimer, and Children, J. A.-H.-T. F., 2016). The changing temperatures caused by the UHI effect lead to different human thermal comfort levels and air qualities, which relate to human health, as well as cooling demands in buildings (Stewart and Oke, 2012; Stone et al., 2010; Vargo et al., 2016).

To consider the combined effect of urban climate change and urbanisation and to assess the spatial vulnerability of the urban population like Nairobi City, advanced climate models are needed. Despite this reality, there is also a challenge that the different interpretation of the term “urban” and “rural” by different scholars has led to vagueness in the use of urban-rural classification in climatological studies, which makes it challenging to determine which factors control the urban climate and therefore more critical in urban landscape planning and climate change management studies (Ng, 2015). UHI investigation has also focused on atmospheric UHI, where the air temperature pattern in urban and rural areas are evaluated based on field measurements. These limited and isolated stationary networks are not capable of capturing various thermal characteristics caused by land use and land cover (LULC) changes (Hu and Brunsell, 2015; Shen et al., 2016). As a result of these, earlier urban climate studies and their potential application (s) to inform policymakers in urban planning and management of land surface temperatures (LSTs) in a city like Nairobi is limited by the lack of systematic criteria for evaluation design and communication of UHI observations, inadequate quantification and irregular description of the city characteristics as they do not show the correlation between urbanisation and urban climate change in the city spatially.

The concept of Local Climate Zones (LCZs) was introduced by Stewart and Oke, 2012 to provide the link between urbanisation and its corresponding thermal impacts on the landscape and to standardise the documentation and global exchange of urban temperature observations (Stewart and Oke, 2012). Each region is identified as a particular class only if the surrounding circles of influence were uniform in surface cover, geometry and human activity (Stewart and Oke, 2012; Bechtel et al., 2015). Unique combinations of these properties provide a distinctive thermal regime for each LCZ, particularly the characteristic temperature regime at screen height, best observed in clear weather conditions and areas of simple relief (Bechtel et al., 2015; Danylo et al., 2016; Stewart and Oke, 2012).

Most recent studies investigating urban temperature fields utilize the LCZ classification and primarily support the correspondence of LCZs with air temperature fields in cities and their surroundings (Bechtel et al., 2015; Geletič and Lehnert, 2016; Lehnert and Geletiˇ, 2016; Lehnert et al., 2015; Stewart and Oke, 2012; Stewart et al., 2014). However, some authors working with LCZs have pointed out that the influence of thermal properties of local climate may significantly vary concerning the geographical location of the zone, the size of the city, the position within the city and relief (Bechtel et al., 2015; Bokwa et al., 2015).

This paper incorporated the concept of LCZ classification to compute and compare the LSTs typical of each LCZs for management of urban heat spots in Nairobi City. The LCZ classification scheme is a useful concept for integrating local climate knowledge into urban planning and design practices since it captures the internal structure and texture of cities to answer some crucial questions about the rapidly urbanising world. These include questions on the adequacy of urban-based adaptation and mitigation policies in response to urban climate change and whether actions in one zone are transferable to another. The results generated from LSTs differentiation based on LCZ classes could be applied in the urban spatial planning and management of SUHI phenomenon; thus, the relevance of the study in an equatorial city like Nairobi.

2. Methodology

2.1. Description of the study area

The study focused on an equatorial city, Nairobi (“city in the sun”) which is the largest (696 km^2) and the capital city in Kenya at a mean altitude of 1684 m above sea level. It is the second-largest city by Populace in the African Great Lakes region after Dar es Salaam in Tanzania with a populace of about 3.36 million according to the year 2011 census estimates (Oyugi et al., 2017). The city started as a rail depot on the Uganda Railway by the colonial authorities in British East Africa in 1899 and became the capital city of Kenya after independence in 1963. The initial city plan which covered 18km^2 and later extended to 25km^2 in 1920 only took into consideration, the European employees of the railway and the European and the Asian traders and completely ignored Asian labourers and Africans which resulted in informal housing on the city perimeter. With functionalism as the main principle, Nairobi city has grown in concentric zones, reflecting the historical stages of its development with clearly-defined historical centres, residential buildings old and new, industrial areas, housing estates, modern shopping centres, malls and allotments, resulting into a neighbourhood with irregular as well as regular (grid and radial grid), and various street plans for the city. However, the plans developed ever since 1927 up to the current Nairobi Integrated Urban Development Master Plan have never been fully realised. There is the presence of a highly polluted river (the Nairobi River) and a higher proportion of open vegetated (low plant) spaces in the city. The landscapes beyond the city's boundaries are predominantly agricultural, with agricultural areas on the Western and sand and bare soils on the Eastern part. Patches of trees (LCZ B) and mixed forests (LCZ A) complete the landscape mosaics of the city (Fig. 1).

2.2. Datasets

For this study, Google earth imagery was used to identify appropriate training sites. Bulk ordering of selected Landsat 8 images (Landsat paths 168 and row 61) from the USGS LandLook data store. The Landsat 8 image quality was 9, and the scene centre was

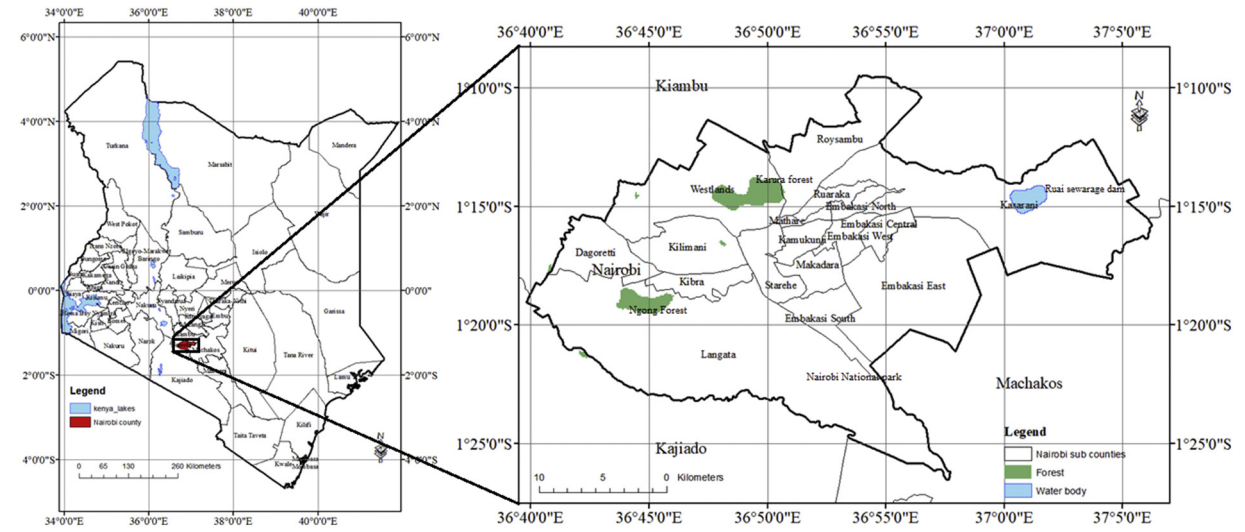

Fig. 1. The Location of Nairobi City.

latitude −1.4483, and longitude 37.0703. Additional processing of Landsat 8 images, including atmospheric correction, was performed on the USGS science for changing world website. In total, six images of processed Landsat 8 data with a spatial resolution of 30 m, with < 10% cloud and haze cover were downloaded from the USGS Earth Explorer interface. Landsat-8 carries two instruments: an operational land imager (OLI) sensor and a thermal infrared sensor (TIRS). The OLI sensor has nine bands (Bands 1–7 and 9 at the 30-m resolution, panchromatic Band 8 at 15-m resolution), while TIRS has two bands (Bands 10 and 11, collected at the 100-m resolution and re-sampled to 30 m). For the interpretation of further analyses carried out in this study, it is important to emphasise that all thermal images were recorded in the morning daylight hours (Table 1).

2.3. Local climate zone classification

The mapping procedure was carried out with the level 0 methodology proposed by the World Urban Database and Access Portal Tools (WUDAPT) (Bechtel et al., 2015), to generates the LCZ map at city scale as follows. In part 1, Google Earth (GE) pro was used to establish the urban domain under study (Known as Region of interest, ROI) and to define areas within the domain that typified LCZ types (Stewart and Oke, 2012). In total, 319 training samples were collected saved in a kmz format. In part 2, Satellite data (Landsat 8) was acquired and processed with System for Automated Geoscientific Analysis (SAGA –GIS). The entire ROI was classified into LCZ types using the training areas provided in part one (Bechtel and Daneke, 2012). The classification was conducted with the built-in random forest tree count of 128 trees and a majority post-filtering with a radius of 5 cells, which was based on the six Landsat 8 images and the training area polygons. The classifier calculated the most likely LCZ type and the probabilities for all LCZ classes for each 100 × 100 m pixel (Bechtel et al., 2015) (Fig. 2).

This method had already been developed and tested (Bechtel et al., 2015; Bechtel and Daneke, 2012; Geletič and Lehnert, 2016; Ren et al., 2016). It is based on the measurable physical properties of the environment and a clearly-defined decision-making algorithm. The algorithm derives from the underlying physical parameters (such as building surface fraction, pervious surface fraction, impervious surface fraction and height of roughness elements) as defined by Stewart and Oke, 2012 (Bechtel and Daneke, 2012).

An accuracy assessment was conducted to check the performance of the random forest classifier and the accuracy of the LCZ classification and to estimate the classification error. Since it was not feasible to check pixel by pixel whether or not the LCZ

Table 1
Landsat 8 Scenes and climatic data (Atmospheric pressure, Air temperature and relative humidity input values) used for LCZ and LST evaluation in Nairobi city.

Scene ID	Acquisition Date	Scene Time (UTC)	Earth-sun Distance	Solar Elevation Angle	Solar Azimuth Angle	Solar Zenith Angle	Atmospheric Pressure (Pa)	Air Temperature (°C)	Relative Humidity (%)
LC81680612013159LGN01	08/06/2013	7:43:01	1.015	54.62	45.01	35.38	84.4	16.75	68.79
LC81680612014034LGN01	03/2/2014	7:44:01	0.986	56.58	118.55	33.42	84.5	21.5	56.4
LC81680612015005LGN01	05/01/2015	7:43:01	0.983	55.23	129.67	34.77	84.5	20.82	43.2
LC81680612016216LGN01	03/08/2016	7:43:01	1.015	56.09	55.07	33.91	84.63	20.53	51.32
LC81680612017362LGN00	28/12/2017	7:43:02	0.983	55.57	131.45	34.43	84.5	21.5	54.87
LC81680612018029LGN00	29/01/2018	7:43:00	0.985	55.93	120.79	34.07	85.54	22.11	39.63

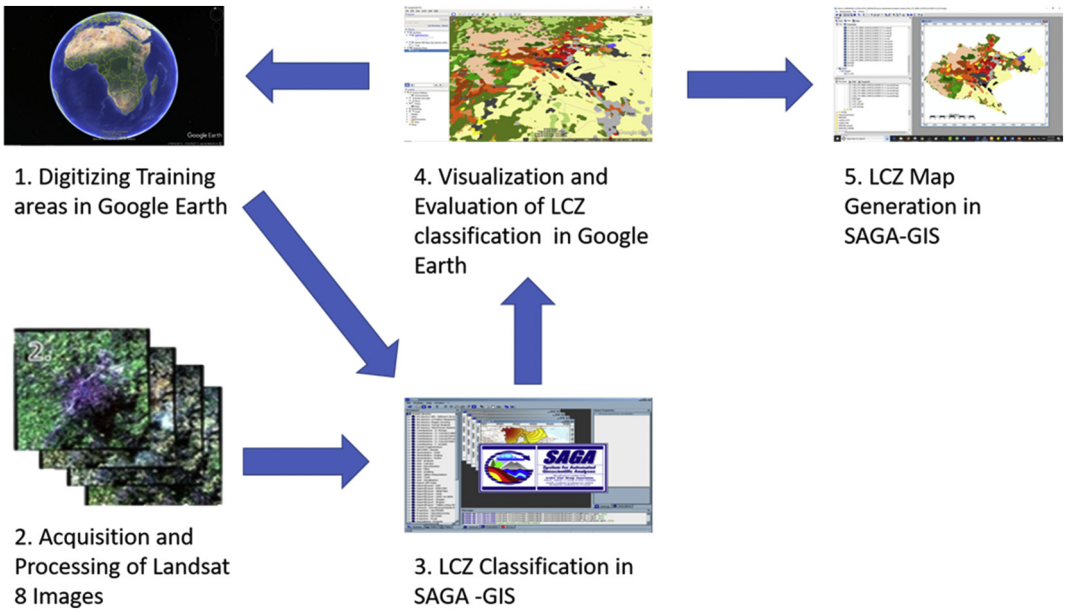

Fig. 2. The workflow of WUDAPT level 0 methodology.

classification was correct, an independent subset of about 50% (Ren et al., 2016), of validation samples for each LCZ class was randomly collected from GE to make an objective comparison and to estimate the classification error. In total, 160 validation samples were collected saved in a kmz format. An assessment that compared the developed LCZ classes with reference data was used to estimate the classification error. The degree of confusion between the classification result and the reference data was summarised in a confusion matrix (Ren et al., 2016). The GE image is regarded as the reference data in this paper which is believed to be accurate enough to reflect the true land-cover to validate the classification result (Fig. 3).

2.4. Land surface temperature

The LST_Landsat_8_split_window toolbox that uses the split-window technique for estimation of surface temperature from daytime Landsat −8 images (Danodia et al., 2017), was used for LST retrieval. The brightness temperature map of thermal bands (band 10, band 11), surface reflectance map of red band (band 4), the normalized difference vegetation index (NDVI) map generated by surface reflectance data, water and cloud mask map, environmental parameters (air temperature, relative humidity and atmospheric pressure) and polygon map of Nairobi city were considered to explicitly to produce LST maps for Nairobi city. The split window algorithm in LST_Landsat_8_split_window toolbox removes the atmospheric effects and obtains the LST from the linear or nonlinear combination of brightness temperatures of two adjacent channels. In total six Landsat images in six different years as shown in Table 1 were used to retrieve and show spatial variations of the current LCZs and LSTs of the city on particular days that excluded extreme weather condition.

2.5. Comparison of land-surface temperatures in local climate zones

To explore the application of LCZ mapping for urban heat characterisation, the thermal analysis was based on the assumption that individual LCZs exhibited characteristic features typical of given LST regime. LST fields were overlaid with LCZs, and typical LSTs were calculated for each zone. Boxplots were used to explore the statistical distribution and the variability of examined LSTs within LCZs for all the six Landsat 8 images. A paired *t*-Test was perfumed to determine if there were mean significant differences between the actual inter LCZ differences in the mean LSTs. The analysis was performed separately for each of the six Landsat 8 temperature fields. Finally, the scores indicating the significance of mean LST differences were summarised in a table.

3. Results

3.1. Local climate zone classifications

The results of WUDAPT level 0 methodology shows maps of the current spatial distribution of the LCZs for Nairobi metropolitan area for different years (Table 1) on particular days that excluded extreme weather condition, based on processed (level 2) Landsat 8 images. All the 17 LCZs (LCZ 1-compact high-rise, LCZ 2-compact mid-rise, LCZ 3-compact low-rise, LCZ 4-open high-rise, LCZ 5-open mid-rise, LCZ 6-open low-rise, LCZ 7-lightweight low-rise, LCZ 8-large low-rise, LCZ 9-sparsely built-up, LCZ 10-heavy industry, LCZ

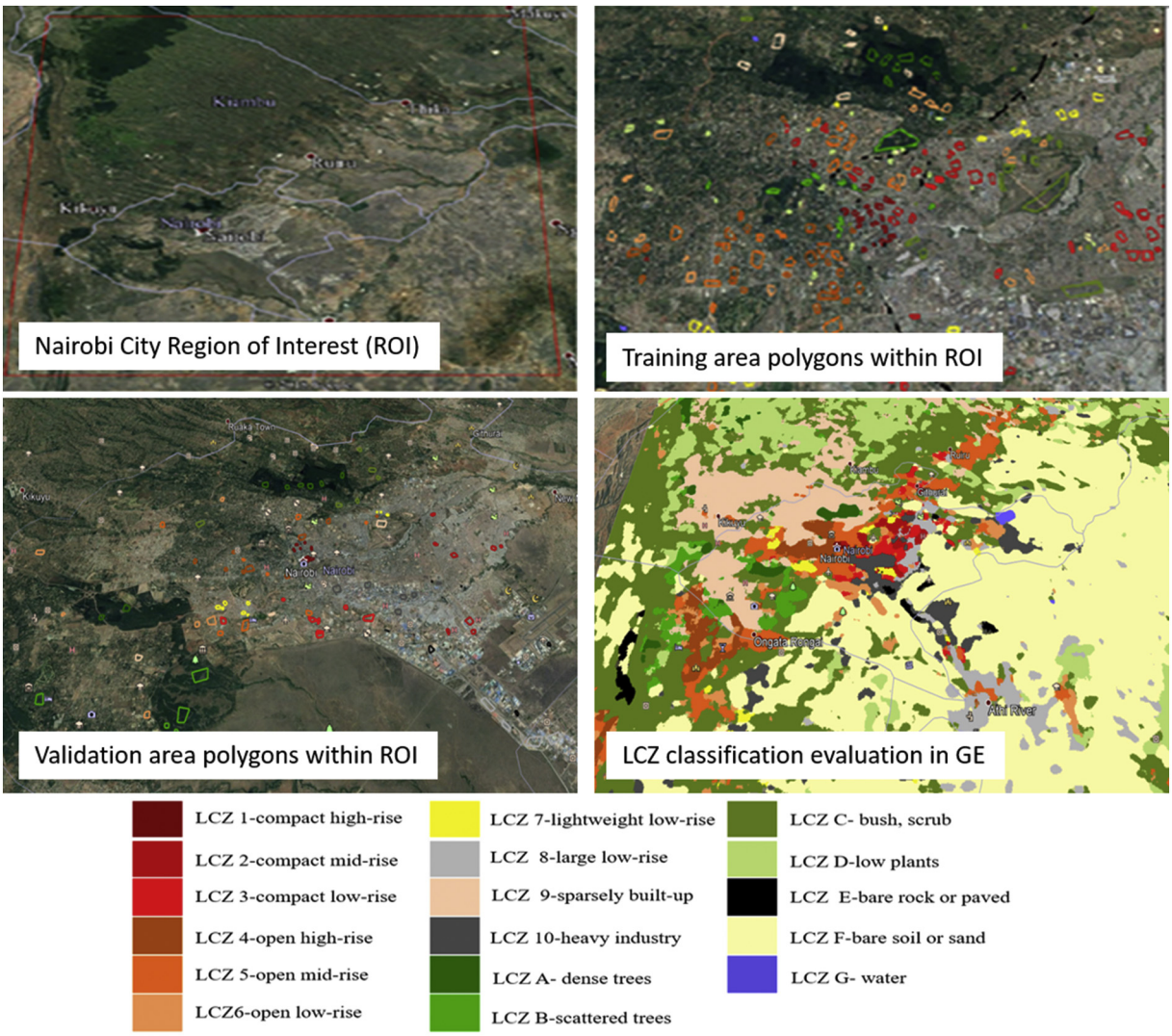

Fig. 3. Location and visualisation of Region of interest, training samples, validation samples, and LCZ classification in Google Earth.

A- dense trees, LCZ B-scattered trees, LCZ C- bush, scrub, LCZ D-low plants, LCZ *E*-bare rock or paved, LCZ F-bare soil or sand; LCZ G-water) are present. There was an agreement between the spatial distribution patterns of the LCZ classes in all the six current LCZ maps generated. The urbanised area (about 60%) was classified into LCZ 1-10, which potentially indicated a larger area of the apparent potential SUHI phenomenon of the city. The highest proportion (17.09%, 8.17%, 6.69% and 5.12%) of the built-up areas was classified as LCZ 9 - Sparsely built (small or medium-sized residential buildings in natural setting with abundance of pervious land cover), LCZ 5 - open midrise (open arrangement of midrise buildings with 3–9 stories and abundance of pervious land cover mostly low plants and scattered trees), LCZ 10 - Heavy industry (low rise and mid-rise industrial structures and abundance of paved land cover with few on no trees), and LCZ 6 - open low-rise (open arrangement of low-rise buildings with 1–3 stories and abundance of pervious land cover mostly low plants and scattered trees), respectively. The Central Business District (CBD) areas of Nairobi city, surrounded by the Uhuru Highway, Haile Selassie Avenue, Moi Avenue, and University Way was in the classes of LCZ 1(compact high rise) (about 0.2%) consisted of high rise density buildings with dense blocks in different heights and with different sky view factor of canyons which demonstrated that the central business centre could also form hot spot areas. Presence of LCZ 7 (Lightweight low-rise) mostly informal settlements (Kibera, Korogocho, Langata, Kangemi, Kawangware, Mathare and Majengo slums) (about 2%) indicated high human vulnerability with adaptive capacity to urban climate impacts in Nairobi's slum community.

The natural areas of Nairobi city belonged to land cover types LCZ A-G. Most natural areas such featureless landscapes of soil and sand with no plants in Syokimau and Mlolongo area, open arrangement of bushes, shrubs and short woody trees mostly on bare soil or sand that cover most parts of Nairobi area, lightly wooded natural landscape Nairobi national park and areas around Ngong and Karura forests and the heavily wooded natural landscape of Ngong and Karura forest, belonged to LCZ F - Bare soil or sand (about 28%), LCZ C -bush, scrub (about 15%) and LCZ B - scattered trees (about 2.%) and LCZ A - Dense trees (about 2.%) respectively. In

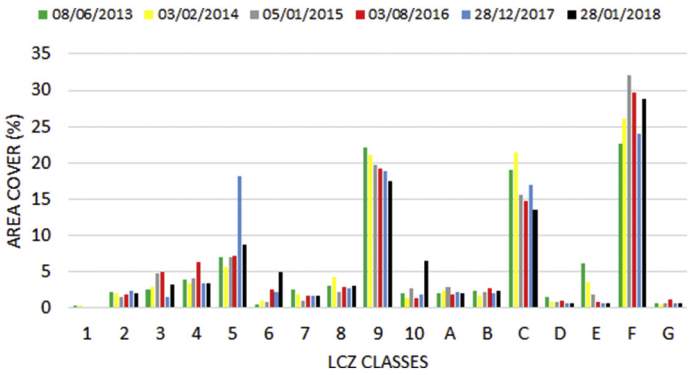

Fig. 4. Percentage of the land cover of LCZs in Nairobi, based on Landsat 8 images. See Table 1.

general, about 50.26% of the Nairobi area was built up while about 49.74% was natural (Figs. 4 & 5).

The overall accuracy was 98.17%, and the Kappa Coefficient was 98.0%. The accuracy assessment demonstrated satisfying results for the WUDAPT level 0 classification. The confusion matrix also indicates that all the LCZs classification a relatively higher accuracy of over 90% for Nairobi city. The misclassification was mainly in built-up types LCZs 2, 6, 8, 9 & 10 (compact midrise, open low rise, large low-rise sparsely built and heavy industry) and land cover types LCZs B, C&G (scattered trees, bush, and water) respectively (Table 2).

3.2. Land surface temperature

All the six Landsat 8 images showed a similar spatial distribution of surface temperatures that were approximately in agreement with the vectorised LCZ boundaries. LST patterns were sensitive to building densities and heights, land cover types and surface wetness. Dry and Natural zones were more thermally responsive (over 45 °C) than wet and built-up zones with vegetation (30 °C - 40 °C). In built-up zones of the city, warmer LSTs (about 45 °C) were very often associated with heavy industry, compact buildings, lightweight low-rise (slums), large low-rise buildings and paved areas (which are quite extensive). While natural LCZs with water bodies, dense trees and sparsely built classes were associated with low LSTs (< 30 °C) regardless of whether they lay in the core of the city or the countryside. Away from the densely built-up areas, the warm parts (about 58 °C) of the cities also occurred near large patches of relatively flat, pervious surfaces (bare soil and sand) in the eastern part of Nairobi which is lying in semi-arid areas of Nairobi. While low LSTs (about 22 °C) occurred at the northern, western and southwestern Nairobi, where the forestry areas prevailed. The coolest LSTs (22 °C) was also correspondent with the water body coverage (e.g., Ruai sewerage treatment dams) (Fig. 6).

3.3. Local climate zones and land surface temperatures

The spatial distributions of LCZs and LSTs indicated that there was a positive degree of correspondence. Therefore, further investigations were performed to assess their relations. Box-plots exploring typical LSTs for individual LCZs showed relatively consistent results for all the six Landsat 8 images considered in this study. However, the LSTs for individual LCZs could not be further compared directly across the different Landsat 8 images as they represented different days of the years spanning from June 2013 to January 2018 (see Table 1). Particular LSTs differences arose out of dynamic factors such as land cover change, and the synoptic situation on a given day. The statistical summary indicated considerable differences among LCZs regarding the mean LSTs of each six Landsat 8 image. LSTs at LCZs 1–10 “built-up cover” types were generally higher than that of LCZs A-G “natural” cover types for the entire city (Fig. 7).

Regarding the LST variation among LCZs with contrasting urban morphology, LCZ 10 (Heavy industry) which is characterised with low rise and midrise (metal, steel and concrete) structures with few or no plants and land cover that is mostly paved and hard parked demonstrated the highest mean LST variation in all the six Landsat 8 images compared to other built-up LCZs. It was followed by LCZ 3 (dense mix of low-rise buildings) and LCZ 2 (compact mid-rise buildings) as the second- and third-warmest LCZs. Additionally, higher mean LSTs were also associated with LCZ 8 (large low-rise) and LCZ 7 (lightweight, low rise) which is mostly slum or surrounded by slum areas whose residents are most vulnerable to the effect of urban climate change. The coolest built-up type LCZ was LCZ 9 (sparsely built with sparse arrangement of small or medium-sized buildings in natural setting and abundance of pervious land cover comprising of both low plants and scattered trees) and LCZ 4 (open high-rise buildings with abundance of pervious land cover constituting of both low plants and scattered trees), due to the vegetation cooling effect. Regarding the LST variation among natural LCZ types, LCZ A (dense trees in a pervious land cover of low plants) and, LCZ G (large open water bodies), demonstrated the lowest mean LSTs. This was followed by LCZ B (scattered trees and pervious land cover of low plants), LCZ C (open arrangements of bushes, scrubs and short woody trees with pervious land cover that is made up of bare soil or sand) and LCZ D (low plants mostly featureless landscape of grass or herbaceous plants, or crops with few or no trees). The natural LCZs functioned as natural forests, tree cultivations, urban parks natural scabland, grassland or. Generally, water bodies and forested areas recorded the lowest mean LSTs in all the six Landsat 8 images (Fig. 8).

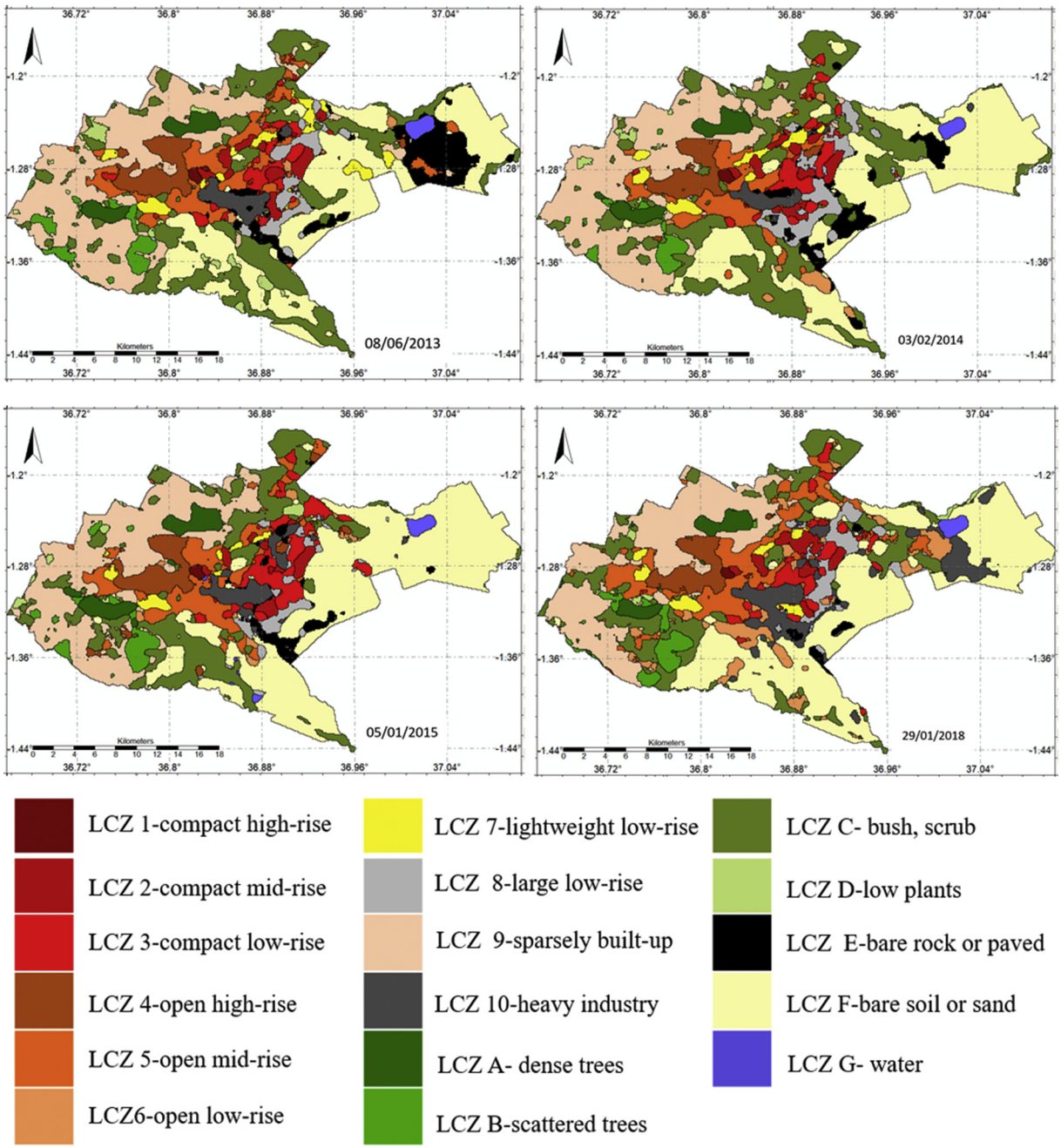

Fig. 5. Spatial distribution of LCZs in Nairobi, based on Landsat 8 images. See Table 1.

From the *t*-Test results, presented in Table 3, there existed statistically significant differences ($P < 0.05$) among mean LSTs between the LCZs in all the six Landsat 8 images. Significant differences in mean LSTs represent positive results in this analysis. This result strongly supports the WUDAPT level 0 methodology used for LCZ classification in Nairobi city.

4. Discussion

4.1. Local climate zone classification

The WUDAPT Level 0 data is a coarse level of data gathering but provided comprehensive and consistent coverage for Nairobi city. This study has been used to describe the urban landscape of Nairobi city regarding neighbourhood-scale using the LCZ scheme as a spatial unit (Bechtel et al., 2015; Bechtel and Daneke, 2012; Stewart and Oke, 2012) using available multi-spectral satellite imagery

Table 2
Confusion matrix of LCZ Map in Nairobi City. See Fig. 3.

LCZ CLASS	LCZ 1	LCZ 2	LCZ 3	LCZ 4	LCZ 5	LCZ 6	LCZ 7	LCZ 8	LCZ 9	LCZ 10	LCZ A	LCZ B	LCZ C	LCZ D	LCZ E	LCZ F	LCZ G	Number of Predicted Pixels	User' Accuracy (%)
LCZ 1	14	0	0	0	0	0	0	0	0	0	0	0	0	0	0	0	0	14	100
LCZ 2	0	32	0	0	0	0	0	0	0	2	0	0	0	0	0	0	0	34	94.1
LCZ 3	0	0	42	0	0	0	0	0	0	0	0	0	0	0	0	0	0	42	100
LCZ 4	0	0	0	44	0	0	0	0	0	0	0	0	0	0	0	0	0	44	100
LCZ 5	0	0	0	0	40	0	0	0	0	0	0	0	0	0	0	0	0	40	100
LCZ 6	0	0	0	0	1	52	0	0	0	0	0	0	0	0	0	0	0	53	98.1
LCZ 7	0	0	0	0	0	0	13	0	0	0	0	0	0	0	0	0	0	13	100
LCZ 8	0	0	0	0	0	0	0	80	0	0	0	0	0	0	1	0	0	81	98.8
LCZ 9	0	0	0	0	0	0	1	0	103	0	0	0	0	0	0	0	0	104	99
LCZ 10	0	0	5	0	0	0	0	0	0	48	0	0	0	0	2	0	0	55	87.3
LCZ A	0	0	0	0	0	0	0	0	0	0	54	0	0	0	0	0	0	54	100
LCZ B	0	0	0	0	0	0	0	0	0	0	0	83	0	0	0	0	4	87	95.4
LCZ C	0	0	0	1	0	0	0	0	0	0	0	0	130	0	0	0	2	133	97.7
LCZ D	0	0	0	0	0	0	0	0	0	0	0	0	0	177	0	0	0	177	100
LCZ E	0	0	0	0	0	0	0	0	0	0	0	0	0	0	7	0	0	7	100
LCZ F	0	0	0	0	0	0	0	0	0	0	0	0	0	0	0	112	0	112	100
LCZ G	0	0	0	0	0	0	0	0	0	0	0	0	0	0	1	0	44	45	97.8
Number of actual pixels	14	32	47	45	41	52	14	80	103	50	54	83	130	177	11	112	50	**Overall Accuracy**	**98%**
Producer's accuracy (%)	100	100	89	98	98	100	93	100	100	96	100	100	100	100	63.6	100	88	**Kapa Coefficient**	**0.98**

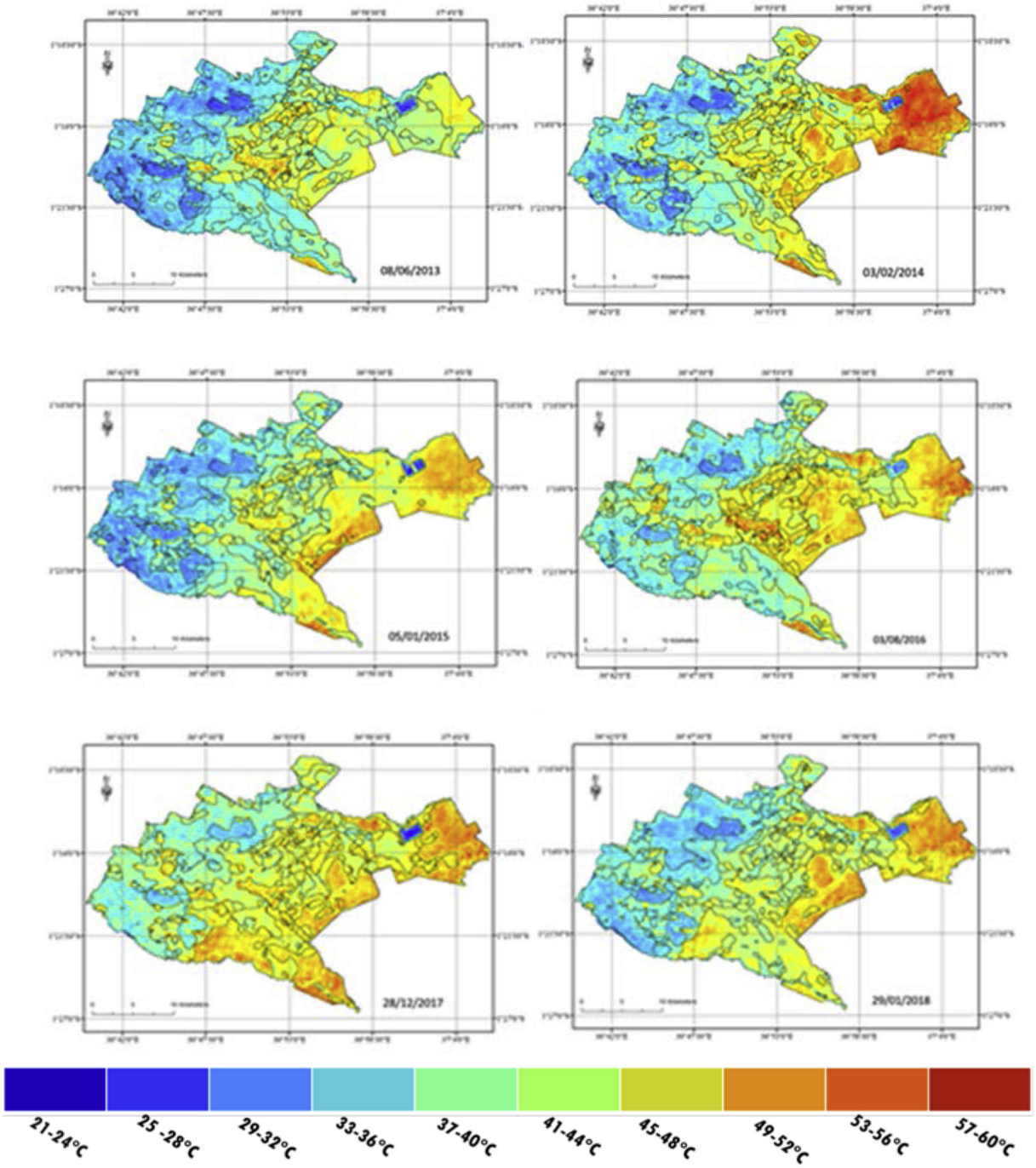

Fig. 6. Spatial distribution and Variability of LST in Nairobi City from six Landsat-8 images. See Table 1 and Fig. 5.

(Landsat 8) and Google Earth in free SAGA_GIS software. Nairobi city urban domain was categorised into ten urban and seven natural LCZs (Urban surface cover types). Each LCZ type was described regarding the typical appearance of each in ground-based and aerial photographs and was linked to some urban parameter values as also described in Stewart and Oke, 2012, Tables 3 and 4 (Bechtel et al., 2015; Stewart and Oke, 2012).

The LCZ classification result of Nairobi city is more reliable and accurate due to the Landsat 8 images with < 10% cloud cover, acquired immediately after the rainy seasons in Nairobi area that eliminated the solar and atmosphere influence. However, the challenge in classification persisted due to limited information about the buildings and vegetation in the Landsat 8 images. The Google Earth image was regarded as the reference data in this study, which is believed to be accurate enough to reflect the true land-

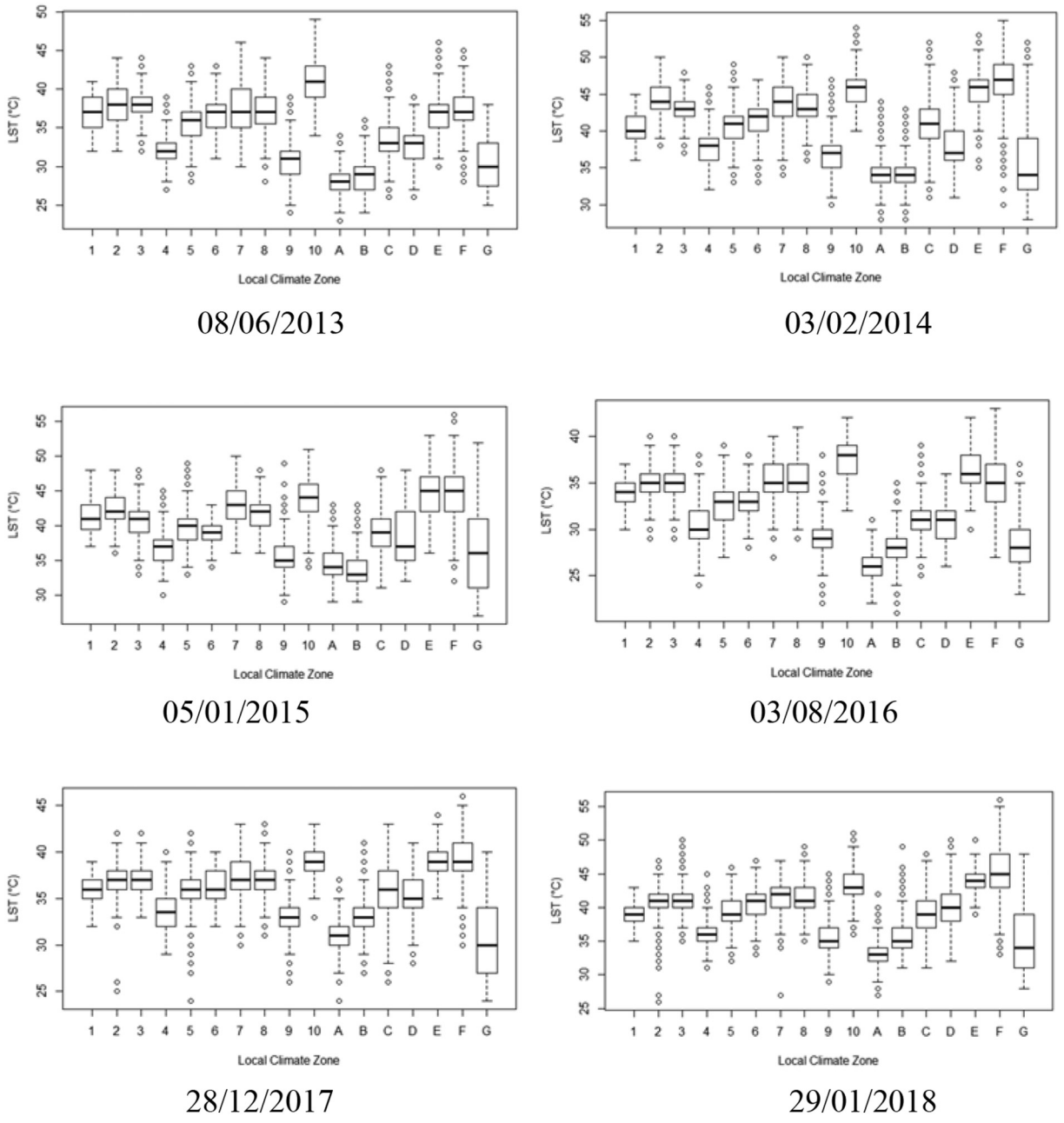

Fig. 7. Boxplots with LSTs in LCZ classes for Nairobi city based on six Landsat 8 images; the line within the box indicates the median. The bottom of the box is the first quartile, and the top is the third quartile. Black boxes crosses indicate outliers.

cover to validate the classification result. The LCZ classification study offers the meaning of the term urban on a measurable basis defined as a 'Local Climate Zone' for standardised assessments to gain further insight into evaluating dynamism of urban morphology of Nairobi city. For instance, the possibility of quantitatively defining the LCZs in Nairobi could open opportunities for domestic and global inter and intra LCZ comparisons between cities, to ensure comprehensive planning and compilation of feasible urban plans. The 17 LCZs should nevertheless be familiar to users (city planners and policymakers) in Nairobi city.

4.2. Land surface temperatures

This analysis indicated specific differences between six Landsat 8 images. Each image leads to different LSTs using the same Split window retrieval algorithm for Landsat 8. The differences could be as a result of different environmental parameters scene viewing geometry, time, distance from the sun, and solar azimuth angle (Krayenhoff & Voogt, 2016) as shown in Table 1. A higher proportion

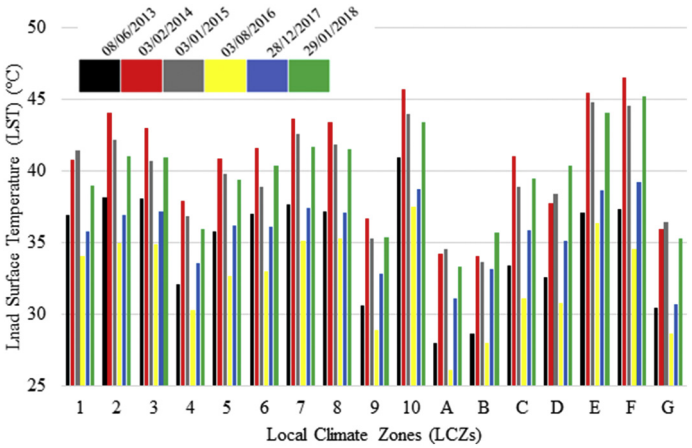

Fig. 8. Mean LST distribution of LCZ classes for Nairobi city based on Landsat 8 images for different Years with urban LCZ types (LCZ 1–10) and natural LCZ types (LCZ A–G). See Table 1 for the scene ID explanation.

Table 3
Results for t-test analysis of LSTs between individual LCZs in six different Landsat 8 images. See Table 1 for the scene ID explanation.

Image date	t-Statistic	*P*-Value	Conf.int
08/06/2013	−7.5683	5.373775e-13	−2.71–1.59
03/02/2014	−4.4191	1.433734e-05	−2.542–0.975
03/01/2015	−4.3615	1.574107e-05	−2.84–1.08
03/08/2016	−12.1647	5.33341e-31	−2.51–1.81
28/12/2017	−13.0012	8.596511e-31	−5.07–3.73
29/01/2018	−13.0155	1.737407e31	−5.83–4.30

of vertically-oriented surfaces in urban areas compared to rural environments causes uneven solar heating of those surfaces and induces a thermal anisotropy effect (Lelovics and Unger, 2013; Unger, 2004; Voogt et al., 1998). It is important to stress that both scenes identified the same sets of warmest (coldest) LCZs. Last, but not least, an essential precondition for LST comparison between different zones is the mutual independence of LCZ classification and the LST fields. Consequently, this is an essential methodological aspect of this study concerning widely-used imagery-based methods (Bechtel et al., 2015; Brousse et al., 2016; Cai et al., 2016; Danylo et al., 2016; Ren et al., 2016; Ren et al., 2017; See et al., 2015; Wang et al., 2018), including thermal bands for LCZ delimitation.

Overlaying a temporal series of thermal satellite imagery with the LCZ boundaries was essential to understand the spatial locations of hotspots in Nairobi city to allow for further examination. The results of the study provided a partial, but coherent, insight into nature of morning hour (around 07.00 h) spatial distribution of LSTs in LCZs as the vertical surfaces was neglected. Knowledge of LSTs as an essential climate parameter, related to surface energy balance is critical in the management of SUHI in Nairobi city. The characteristics of UHI are related to both the intrinsic nature of a city such as increased roughness due to building geometries, drier and more impervious surfaces and anthropogenic heat and moisture releases (Stewart and Oke, 2012; Bechtel et al., 2015), as well as to external influences which originate from climate, prevailing weather circumstances and seasons (Bechtel et al., 2015; Connor et al., 2015; See et al., 2015; Stewart and Oke, 2006; Iain D. Stewart et al., 2014). While it is mostly a nocturnal phenomenon, SUHI occurs during the daytime with a spatial and temporal pattern actively controlled by the unique characteristics of each LCZs (Bokva et al., 2014; Gulyás et al., 2006; Ragheb et al., 2016; Unger et al., 2014). It is typically developed during clear skies and is ordinarily an aftereffect of the dominant reflective surfaces of the city compared to surrounding rural areas (Ching et al., 2016; Stewart et al., 2014; Stone and Rodgers, 2001). Thus LSTs retrieved from Landsat 8 (which has a Thermal Infrared Sensor (TIRS) that captures the temperatures of the Earth's surface in band 10 and band 11 with a spatial resolution of 100 m), maybe a suitable alternative, as their spatial coverage is complete. Even though surface temperature influences the air temperature of the boundary layer atmosphere (Unger, 2004), the interaction between the two types of temperatures is quite complicated in urban settings (Schwarz et al., 2012), The spatial extent of LSTs are modified by several static factors (for example LULC types, urban morphology, topography) as defined by the LCZ classification and dynamic factors (for example geometry of thermal imagery acquisition, solar elevation) as defined by the sensor. These factors modify the energy balance of urban areas and also generate thermal anisotropy effects (Bechtel et al., 2012).

When interpreting the thermal behaviour of LCZ 10, it must be taken into account that the LCZ 10 delineation was based on the Nevertheless, the higher LSTs of industrial areas in daytime which have previously been described by many authors (Buyantuyev and Ecology, 2010; Li et al., 2012; Stewart et al., 2014; Taubenböck et al., 2010; Voogt and Oke, 2003; Voogt et al., 1998). Unexpectedly, the LSTs of LCZ 8 (large low-rise) were in all the scenes considerably lower than the LSTs of LCZ 10. This may correspond to the different thermal properties implicit in the large roof surfaces that occur quite often in LCZ 8 (Akbari and Levinson, 2008; Bechtel

et al., 2015; Parlow et al., 2014). LCZ A (dense trees) was identified as a lower LST zone, but a large number of positive outliers are evident (i.e., highest LST). This is a reaction to the relatively high number of patches, mostly consisting of clear-cuts of areas that are quite often below the spatial resolution of the data used for LCZ classification. On the other hand, the low LST of LCZ G (water) should be considered as realistic, since temperature differences reflect the different characters of individual bodies of water.

Therefore, there are several criteria could be used to identify and control urban heat loads in Nairobi city which should be investigated: the (H/W) ratio between the height of the buildings (H) and the width of the adjacent street (W), the orientation, reflectivity, conductivity, plot coverage, balconies and vegetation building heights, and human activities (Bechtel et al., 2019; Li et al., 2018; Taslim et al., 2015).

Emission from heat sources together with heat accumulated and reradiated back into the environment, leads to higher LSTs in built-up LCZs such as industrial areas LCZ 10 (heavy industry). The increased temperatures are anticipated to bring significant heat waves throughout urban areas in Nairobi. Most affected will be areas which have had vegetation removed and in places of dark surfaces such as asphalt roads and black roofs. Other factors contributing to the SUHI include reduced porous surfaces, tall buildings and narrow streets, decreased surface waters, and concentrating of heat-generating activities in urban areas, e.g. motor vehicles, factories and homes. Therefore, mitigation and adaptation strategies that increase urban green cover (dense trees), pervious land cover (low plants and grasslands) low albedo of materials (light coloured surfaces) and reducing dense development (to significantly reduce the increase in shaded area with building height) (Bechtel et al., 2017; Buyantuyev and Wu, 2010; Connor et al., 2015; See et al., 2015; Voogt and Oke, 2003) is critical for Nairobi city.

4.3. Urban planning and design strategies to manage urban heat in Nairobi City

The application of the findings to the current urban planning and design could be critical, as part of the road map to full realisation of the Nairobi city plans developed ever since 1927 up to the current Nairobi Integrated Urban Development Master Plan. Transforming the existing urban landscape while designing new buildings and infrastructure to the highest standards informed by climate science requires a new agency and ambition of urban design and planning to create a healthier urban environment through appropriate, climate-informed design. Presented in this section are the four main adaptive design strategies for urban planning and design in Nairobi city that could work to prepare for the adverse impacts of hot temperatures, while also adapting to current urban heat loads with a substantial expected increase in urban heat intensities in coming years. They include: improving the efficiency of urban systems, both in energy and transportation; optimising the form and layout of urban districts to enhance ventilation; promoting appropriate building materials with high reflectivity and; increasing the use of green and blue urban infrastructure.

4.3.1. Sustainable and efficient urban systems

There is a need to evaluate the sources of waste heat from urban functions and systems in Nairobi city and to prioritise the best approaches for mitigating them. For example, the waste heat from mechanical systems can be recovered to produce energy or hot water. The ideas for reducing travel by cars into Nairobi city could include congestion pricing policies, the creation of protected bike lanes and wider sidewalks, and ultimately, convenient, rapid transit alternatives (Joyce et al., 2017; Kaloustian et al., 2016; Villanueva-Solis, 2017).

4.3.2. Urban form and layout

The orientation and the height of buildings have a significant impact on their surrounding local microclimates. These morphological factors control how wind moves through the city's streetscape. During hot days, wind breezes are often blocked by buildings. Microscale passive cooling strategies to enhance ventilation through the use of linear parks and wind corridors can improve the quality of life during the hot season. As urban redevelopment proceeds, the creation of varied building heights and massing, rather than a monolithic wall of highrise buildings, could help to mitigate the buildup of daytime urban heat in Nairobi's high-rise buildings (Bechtel and Daneke, 2012; Joyce et al., 2017; Kaloustian and Bechtel, 2016; Taslim et al., 2015).

4.3.3. Construction materials

The thermal behaviour of materials used for building envelopes and urban streets influences the magnitude of the heat island effect. Asphalt and concrete tend to absorb the sun's heat during daytime and reradiate that heat during the night. In contrast, cool roofing materials are reflective and emissive. The heat mitigation strategies that could be used by Nairobi city based on properties of construction materials include high albedo reflective roof coatings, green roofs, and reflective or permeable pavements (Joyce et al., 2017; Taslim et al., 2015).

4.3.4. Green infrastructure

One of the most critical design approaches for urban cooling is the use of “blue and green” infrastructure. Due to evaporative cooling and their ability to shade sidewalks, buildings and the intake of air into buildings, trees and other vegetation decrease the heating of buildings, pedestrians, and the urban landscape. Other green infrastructure innovations, including bioswales, green roofs, and urban forestry, are increasingly deployed by cities to reduce polluted storm runoff and flooding, to filter air pollutants, and to benefit public health and quality of life. In Nairobi's CBD, vegetation could take multiple forms: green roofs and walls, street trees, and newly created linear parks using privately-owned public space (Bechtel et al., 2019; Kaloustian et al., 2016; Li et al., 2018; Taslim et al., 2015; Villanueva-Solis, 2017).

5. Conclusion

The study was the first to compare the inter LCZ differentiation of LSTs distribution in Nairobi, which is a tropical city, employing data provided by the Landsat 8 sensor. There was a positive correspondence in the spatial distributions of LCZs and LSTs under the limited relief and weather conditions tested in this study. The division of urban and rural landscapes into LCZs is therefore justified on both physical and empirical grounds. LSTs show typical surface temperatures that differ significantly between LCZs. The warm zones were LCZ 10 (heavy industry), LCZ 3 (compact low-rise buildings), LCZ 2 (compact mid-rise buildings), LCZ 7 (lightweight low-rise) and LCZ 8 (large low-rise) while the cool zones (LCZ G (water bodies), LCZ A (dense trees) and LCZ 9 (sparsely built). These findings generally support the concept of LCZs as a classification unit for urban studies and future spatial planning in Nairobi city. Although the concept of LCZs was developed for the classification of air temperature measurements, the results of this paper confirm that individual LCZ also prove characteristic features of LSTs. Specific questions, such as seasonality in LST differences and thermal anisotropy (complete surface temperature differences), remain open to future research. In conclusion, application of climate science to the urban planning and design of Nairobi city could lead to the full realisation of the city plans developed ever since 1927 up to the current Nairobi Integrated Urban Development Master Plan.

Declaration of Competing Interest

The authors have no conflict of interest.

Acknowledgements

The project leading to this application has received funding from the ERA-net LOCLIM_3 project Fund and Africa-ai-Japan project fund. The authors thank USGS (U.S. Geological Survey) for the free data availability and SAGA GIS and Google Earth pro Developers for the free software. Special thanks to the LCZ scheme developers for giving their advice on applying the LCZ scheme and adopting the WUDAPT method in this study.

References

Akbari, H., Levinson, R., 2008. Evolution of cool-roof standards in the US. Adv. Build. Energy Res. 2 (1), 1–32. https://doi.org/10.3763/aber.2008.0201.

Angel, S., Sheppard, S.C., Civco With Robert Buckley, D.L., Chabaeva, A., Gitlin, L., Kraley, A., ... Perlin, M., 2005. The Dynamics of Global Urban Expansion. Retrieved from. http://www.williams.edu/Economics/UrbanGrowth/DataEntry.htm.

Bechtel, B., Daneke, C., 2012. Classification of local climate zones based on multiple earth observation data. IEEE J. Select. Topics Appl.Earth Observ. Remote Sens. 5 (4), 1191–1202. https://doi.org/10.1109/JSTARS.2012.2189873.

Bechtel, B., Zakšek, K., Hoshyaripour, G., 2012. Downscaling land surface temperature in an urban area: a case study for Hamburg, Germany. Remote Sens. 4 (10), 3184–3200. https://doi.org/10.3390/rs4103184.

Bechtel, B., Alexander, P., Böhner, J., Ching, J., Conrad, O., Feddema, J., ... Stewart, I., 2015. Mapping local climate zones for a worldwide database of the form and function of cities. ISPRS Int. J. Geo Inf. 4 (1), 199–219. https://doi.org/10.3390/ijgi4010199.

Bechtel, B., Demuzere, M., Sismanidis, P., Fenner, D., Brousse, O., Beck, C., ... Verdonck, M.-L., 2017. Quality of crowdsourced data on urban morphology—the human influence experiment (HUMINEX). Urban Sci. 1 (2), 15. https://doi.org/10.3390/urbansci1020015.

Bechtel, B., Alexander, P.J., Beck, C., Böhner, J., Brousse, O., Ching, J., ... Xu, Y., 2019. Generating WUDAPT level 0 data – current status of production and evaluation. Urban Clim. 27 (October 2018), 24–45. https://doi.org/10.1016/j.uclim.2018.10.001.

Bokva, A., Dobrovolny, P., Gál, T., Geletic, J., Gulyás, Á., Hajtó, M., ... Zuvela-Aloise, M., 2014. Modelling the Impact of Climate Change on heat Load Increase in Central European cities, (Sievers 1995). pp. 6–10. Retrieved from. http://real.mtak.hu/28567/1/CCMA2-5-3151332_a.pdf.

Bokwa, A., Hajto, M.J., Walawender, J.P., Szymanowski, M., 2015. Influence of diversified relief on the urban heat island in the city of Kraków, Poland. Theor. Appl. Climatol. 122 (1–2), 365–382. https://doi.org/10.1007/s00704-015-1577-9.

Brousse, O., Martilli, A., Foley, M., Mills, G., Bechtel, B., 2016. WUDAPT, an efficient land use producing data tool for mesoscale models? Integration of urban LCZ in WRF over Madrid. Urban Clim. 17, 116–134. https://doi.org/10.1016/j.uclim.2016.04.001.

Buyantuyev, A., Ecology, J.W.-L., 2010. Undefined. (n.d.). Urban heat Islands and Landscape Heterogeneity: linking Spatiotemporal Variations in Surface Temperatures to land-cover and Socioeconomic Patterns. Springer Retrieved from. https://idp.springer.com/authorize/casa?redirect_uri=https://link.springer.com/article/10.1007/s10980-009-9402-4&casa_token=evhNKOemkdYAAAAA:4STOLOYd7fEorj1NaYQ2ABFIH-oA0WRkaDFniNUSjEJxSnWedLyvVPPzRcaiC1-8ZmgLWOENmQk_NCxM7Q.

Buyantuyev, Alexander, Wu, J., 2010. Urban heat islands and landscape heterogeneity: linking spatiotemporal variations in surface temperatures to land-cover and socioeconomic patterns. Landsc. Ecol. 25 (1), 17–33. https://doi.org/10.1007/s10980-009-9402-4.

Cai, M., Ren, C., Xu, Y., Dai, W., Wang, X.M., 2016. ScienceDirect local climate zone study for sustainable megacities development by using improved WUDAPT methodology – a case study in Guangzhou. Procedia Environ. Sci. 36, 82–89. https://doi.org/10.1016/j.proenv.2016.09.017.

Ching, J., Mills, G., See, L., Bechtel, B., Feddema, J., Stewart, I., ... Masson, V., 2016. Wudapt (world urban database and access portal tools): an international collaborative project for climate relevant physical geography data for the world ' S. Cities 1–7.

Connor, O., De Fatima, M., Bechtel, B., Foley, M., Mills, G., Ching, J., ... Gál, T., 2015. CENSUS of Cities: LCZ Classification of Cities (Level 0) – Workflow and Initial Results from Various Cities. ICUC9, Toulouse, France, pp. 8–13. https://doi.org/10.13140/RG.2.1.4028.5206. (20–24 July), (Level 0).

Danodia, A., Nikam, B.R., Kumar, S., 2017. Land Surface Temperature Retrieval by Radiative Transfer Equation and Single Channel Algorithms Using Landsat-8 Satellite Data Land Surface Temperature Retrieval by Radiative Transfer Equation and Single Channel Algorithms Using Landsat-8 Satellite, (October).

Danylo, O., See, L., Bechtel, B., Schepaschenko, D., Fritz, S., 2016. Contributing to WUDAPT: a local climate zone classification of two cities in Ukraine. IEEE J. Select. Topics Appl.Earth Observ. Remote Sens. 9 (5), 1841–1853. https://doi.org/10.1109/JSTARS.2016.2539977.

Geletič, J., Lehnert, M., 2016. GIS-based delineation of local climate zones: the case of medium-sized central European cities. Moravian Geogr. Rep. 24 (3), 2–12. https://doi.org/10.1515/mgr-2016-0012.

Gulyás, Á., Unger, J., Matzarakis, A., 2006. Assessment of the microclimatic and human comfort conditions in a complex urban environment: modelling and measurements. Build. Environ. 41 (12), 1713–1722. https://doi.org/10.1016/J.BUILDENV.2005.07.001.

Hashim, J.H., Hashim, Z., 2016. Climate change, extreme weather events, and human health implications in the Asia Pacific region. Asia Pac. J. Public Health 28 (2_suppl), 8S–14S. https://doi.org/10.1177/1010539515599030.

Hu, L., Brunsell, N.A., 2015. A new perspective to assess the urban heat island through remotely sensed atmospheric profiles. Remote Sens. Environ. 158, 393–406. https://doi.org/10.1016/J.RSE.2014.10.022.

Joyce, B., Rosenthal, K., Raven, J., 2017. Urban Heat and Urban Design — An Opportunity to.
Kaloustian, N., Bechtel, B., 2016. Local climatic zoning and urban Heat Island in Beirut. Procedia Eng. 169, 216–223. https://doi.org/10.1016/j.proeng.2016.10.026.
Kaloustian, N., Bitar, H., Diab, Y., 2016. Urban Heat Island and urban planning in Beirut. Procedia Eng. 169, 72–79. https://doi.org/10.1016/j.proeng.2016.10.009.
Krayenhoff, E., Voogt, J., 2016). Daytime thermal anisotropy of urban neighbourhoods: morphological causation. Remote. Sens. 8 (2), 108.
Lehnert, M., Geleti˘, J., 2016. Land Surface Temperature Differences within Local Climate Zones, Based on Two Central European Cities Land Surface Temperature Differences within Local Climate Zones, Based on Two Central European Cities, (September). https://doi.org/10.3390/rs8100788.
Lehnert, M., Geletič, J., Husák, J., Vysoudil, M., 2015. Urban field classification by "local climate zones" in a medium-sized central European city: the case of Olomouc (Czech Republic). Theor. Appl. Climatol. 122 (3–4), 531–541. https://doi.org/10.1007/s00704-014-1309-6.
Lelovics, E., Unger, J., 2013. Mapping local climate zones with a vector-based gis method. Air & Water Comp. Environ. Aerul Si Apa Compone 423–430.
Li, Y., Zhang, H., Kainz, W., 2012. Monitoring patterns of urban heat islands of the fast-growing Shanghai metropolis, China: using time-series of Landsat TM/ETM+ data. Int. J. Appl. Earth Obs. Geoinf. 19, 127–138. https://doi.org/10.1016/J.JAG.2012.05.001.
Li, H., Zhou, Y., Li, X., Meng, L., Wang, X., Wu, S., Sodoudi, S., 2018. A new method to quantify surface urban heat island intensity. Sci. Total Environ. 624, 262–272. https://doi.org/10.1016/j.scitotenv.2017.11.360.
Ng, Y., 2015. A study of urban Heat Island using "local climate zones" – the case of Singapore. British J. Environ. Clim. Change 5 (2), 116–133. https://doi.org/10.9734/BJECC/2015/13051.
Oppenheimer, M., Children, J. A.-H.-T. F, 2016. Children and Climate Change. Princeton University, Spring Vol. 26, No. 1. https://www.jstor.org/stable/43755228.
Oyugi, M.O., Odenyo, V.A.O., Karanja, F.N., 2017. The implications of land use and land cover dynamics on the environmental quality of Nairobi City. Kenya 6 (3), 111–127. https://doi.org/10.5923/j.ajgis.20170603.04.
Parlow, E., Vogt, R., Feigenwinter, C., 2014. The urban heat island of Basel – seen from different perspectives. DIE ERDE – J. Geogr. Soc. Berlin 145 (1–2), 96–110. Retrieved from. https://www.die-erde.org/index.php/die-erde/article/view/95.
Ragheb, A.A., El-Darwish, I.I., Ahmed, S., 2016. Microclimate and human comfort considerations in planning a historic urban quarter. Int. J. Sustain. Built Environ. 5 (1), 156–167. https://doi.org/10.1016/j.ijsbe.2016.03.003.
Ren, C., Cai, M., Wang, M., Xu, Y., Ng, E., 2016. Local climate zone (LCZ) classification using the world urban database and access portal tools (WUDAPT) method: A case study in Wuhan and Hangzhou. In: The Fourth International Conference on Countermeasure to Urban Heat Islands (4th IC2UHI), (May), pp. 1–12.
Ren, C., Fung, J.C.-H., Tse, J.W.P., Wang, R., Wong, M.M.F., Xu, Y., 2017. Implementing WUDAPT product into urban development impact analysis by using WRF simulation result - a case study of the Pearl River Delta Region (1980–2010). In: Proceedings of the 13th Symposium on Urban Environment, pp. 22–26. January. Retrieved from. http://files/3490/REN et al. - 9.2 Implementing WUDAPT product into urban develop.pdf.
Santamouris, M., Paraponiaris, K., Mihalakakou, G., 2007. Estimating the ecological footprint of the heat island effect over Athens, Greece. Clim. Chang. 80 (3–4), 265–276. https://doi.org/10.1007/s10584-006-9128-0.
Santamouris, Mat, Haddad, S., Fiorito, F., Osmond, P., Ding, L., Prasad, D., ... Wang, R., 2017. Urban Heat Island and overheating characteristics in Sydney, Australia. An analysis of multiyear measurements. Sustainability 9 (12), 712. https://doi.org/10.3390/su9050712.
Schwarz, N., Schlink, U., Franck, U., Großmann, K., 2012. Relationship of land surface and air temperatures and its implications for quantifying urban heat island indicators—an application for the city of Leipzig (Germany). Ecol. Indic. 18, 693–704. https://doi.org/10.1016/J.ECOLIND.2012.01.001.
See, L., Perger, C., Duerauer, M., Fritz, S., Bechtel, B., Ching, J., ... Masson, V., 2015. Developing a community-based worldwide urban morphology and materials database (WUDAPT) using remote sensing and crowdsourcing for improved urban climate modelling. In: 2015 Joint Urban Remote Sensing Event (JURSE). IEEE, pp. 1–4. https://doi.org/10.1109/JURSE.2015.7120501.
Shen, H., Huang, L., Zhang, L., Wu, P., Zeng, C., 2016. Long-term and fine-scale satellite monitoring of the urban heat island effect by the fusion of multi-temporal and multi-sensor remote sensed data: a 26-year case study of the city of Wuhan in China. Remote Sens. Environ. 172, 109–125. https://doi.org/10.1016/J.RSE.2015.11.005.
Stewart, I., Oke, T., 2006. Thermal Differentiation of Local Climate Zones Using Temperature Observations from Urban and Rural Field Sites, (Figure 1).
Stewart, I.D., Oke, T.R., 2012. Local climate zones for urban temperature studies. Bull. Am. Meteorol. Soc. 93 (12), 1879–1900. https://doi.org/10.1175/BAMS-D-11-00019.1.
Stewart, Iain D., Oke, T.R., Krayenhoff, E.S., 2014. Evaluation of the 'local climate zone' scheme using temperature observations and model simulations. Int. J. Climatol. 34 (4), 1062–1080. https://doi.org/10.1002/joc.3746.
Stone, B., Rodgers, M.O., 2001. Urban form and thermal efficiency: how the Design of Cities Influences the Urban Heat Island Effect. J. Am. Plan. Assoc. 67 (2), 186–198. https://doi.org/10.1080/01944360108976228.
Stone, B., Hess, J.J., Frumkin, H., 2010. Urban form and extreme heat events: are sprawling cities more vulnerable to climate change than compact cities? Environ. Health Perspect. 118 (10), 1425–1428. https://doi.org/10.1289/ehp.0901879.
Taslim, S., Parapari, D.M., Shafaghat, A., 2015. Urban design guidelines to mitigate urban heat island (UHI) effects in hot-dry cities. J. Teknologi 74 (4), 119–124. https://doi.org/10.11113/jt.v74.4619.
Taubenböck, H., Esch, T., Wurm, M., Roth, A., Dech, S., 2010. Object-based feature extraction using high spatial resolution satellite data of urban areas. J. Spat. Sci. 55 (1), 117–132. https://doi.org/10.1080/14498596.2010.487854.
Unger, J., 2004. Intra-urban relationship between surface geometry and urban heat island: review and new approach. Clim. Res. 27 (3), 253–264. https://doi.org/10.3354/cr027253.
Unger, János, Lelovics, E., Gál, T., Bulletin, H.G., Unger, J., Lelovics, E., Gál, T., 2014. Local climate zone mapping using GIS methods in Szeged. Hungarian Geographical Bulletin 63 (1), 29–41. https://doi.org/10.15201/hungeobull.63.1.3.
Vargo, J., Stone, B., Habeeb, D., Liu, P., Russell, A., 2016. The Social and Spatial Distribution of Temperature-Related Health impacts from Urban heat Island Reduction Policies. https://doi.org/10.1016/j.envsci.2016.08.012.
Villanueva-Solis, J., 2017. Urban Heat Island mitigation and urban planning: the case of the Mexicali, B. C. Mexico. Am. J. Clim. Chang. 06 (01), 22–39. https://doi.org/10.4236/ajcc.2017.61002.
Voogt, J., Oke, T., 2003. Thermal remote sensing of urban climates. Remote Sens. Environ. 86 (3), 370–384. https://doi.org/10.1016/S0034-4257(03)00079-8.
Voogt, J.A., Oke, T.R., Voogt[2], J.A., 1998. Effects of urban surface geometry on remotely-sensed surface temperature. Int. J. Remote Sens. 19 (5), 895–920. https://doi.org/10.1080/014311698215784.
Wang, R., Ren, C., Xu, Y., Lau, K.K.-L., Shi, Y., 2018. Mapping the local climate zones of urban areas by GIS-based and WUDAPT methods: a case study of Hong Kong. Urban Clim. 24, 567–576. https://doi.org/10.1016/j.uclim.2017.10.001.